Dynamic Stability of Soil-Reinforced Walls

JOHN VRYMOED

A method is developed to determine the static and dynamic stability of soil-reinforced walls. The method determines factors of safety against pullout and yield of the reinforcement and against the wall sliding on its base. These factors of safety are determined as a function of different levels of acceleration applied at the base of the wall. Results are shown when the proposed method was used to determine the stability of a 62-ft high wall constructed as part of the realignment of State Highway 101 in northern California.

The California Department of Transportation (Caltrans) has investigated the various aspects of soil-reinforced walls during the past decade subsequent to Vidal's pioneering in this area (*1*). Because of the great potential oif soil-reinforced walls in reducing the cost of transportation-related construction, Caltrans actively promotes their use when site conditions are favorable. The design and construction of these walls is relatively simple and the procedures are now familiar to many in the profession. In California, one of the inevitable facts of building soil-reinforced walls is the high levels of acceleration that need to be considered for the majority of sites. This is why a practical method and guide was sought that would easily determine the adequacy of any given design under both static and dynamic load conditions.

PREVIOUS INVESTIGATIONS

The first known investigation into the behavior of soil-reinforced earth walls under dynamic load conditions was done by Richardson and Lee (*2*) in 1975. In their investigation, small model walls were constructed and subjected to horizontal accelerations generated by a shaking table. The results of these model tests suggested that the tie forces could be defined by a straightline envelope as a function of horizontal acceleration. To obtain this horizontal acceleration, the use of response spectra and modal participation factors was recommended.

Additional shake table tests on small model walls were carried out by Wolfe et al. (*3*) to determine the effect of vertical accelerations on the tie force and wall displacements. It was concluded from the test results, that for walls having low strain frequencies greater than the dominant frequencies of vibration, the effect of the vertical component of acceleration could be ignored.

Richardson et al. (*4*) conducted field studies on a full scale 20-ft-high wall to test and improve the recommended seismic design derived from the earlier model studies. The field studies used mechanical vibrators and explosives to subject the wall to different levels of excitation. The mechanical vibrators were only able to induce relatively low maximum shear strains of less than 0.001 percent. The explosives, however, induced large strains with associated peak accelerations in excess of 0.5 g at the top and bottom of the wall. The strain resulted in a permanent outward movement of 5 percent of wall height. The dynamic tie forces measured during the explosive tests were much less than the forces predicted by the seismic design based on the small model tests. Because of this discrepancy, the seismic design was revised by Richardson (*5*) to reproduce the tie forces observed in the explosive tests. To accomplish this, the modal participation factors for the first and second mode of vibration were reduced from the earlier recommended values.

This revised design procedure was used by McKittrick and Wojciechowski (*6*) in the design of five soil-reinforced walls at Valdez, Alaska. The structures were designed to withstand a magnitude 8.5 earthquake with associated peak spectral accelerations of 0.5 g and 0.71 g for the first and second modes, respectively. The consequence of incorporating the dynamic forces was to increase the density of reinforcement near the top of the walls.

PROPOSED SEISMIC DESIGN

The proposed seismic design is a pseudo-static method of analysis that treats the wall as a rigid block and treats the soil retained behind the wall as a rigid wedge. This method circumvents the need to determine the primary and secondary modes and the associated modal participation factors as proposed by previous investigators.

The analysis described herein determines the factors of safety as a function of horizontally applied accelerations for both the internal and external stability of a given wall design. Having determined this function, Newmark's method (*7*) is then used to estimate permanent wall displacements. If it is determined that the displacements are excessive for a given wall design and site-specific seismic parameters, the design can be revised and checked again. This seismic design methodology is similar to the method developed by Richards and Elms (*8*) for gravity retaining walls.

The displacements computed by the proposed method are considered to occur by sliding at the base of the wall and/or by pullout of the reinforcing elements causing an outward tilting of the wall face. Total collapse of the wall would be predicted if the factors of safety against yield of the elements were to drop below unity.

California Department of Transportation, Office of Transportation Laboratory, 5900 Folsom Boulevard, Sacramento, Calif. 95819.

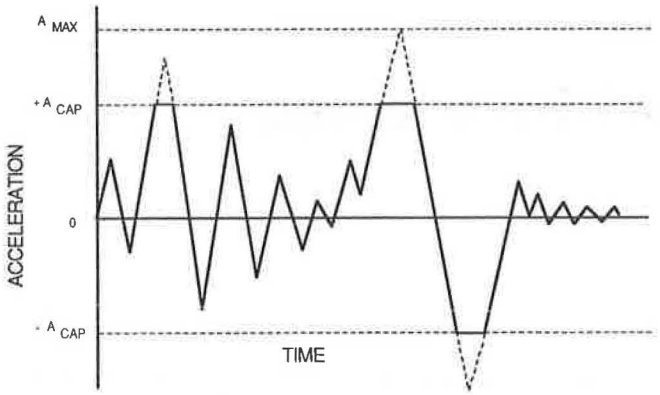

FIGURE 1 Capped acceleration time history.

Because the wall is analyzed for both internal and external stability, the acceleration that a given level of reinforcement experiences may be less than the input acceleration if that acceleration causes sliding to occur at the base of the wall and/or causes the reinforcement below that level to exceed its pullout resistance. Therefore, a given level of reinforcement may experience an acceleration time history which is "capped" as shown in Figure 1. Franklin and Chang (*9*) reported variations of standardized displacements with ratios of critical and peak accelerations. These displacements were computed from acceleration and velocity time histories scaled to peak values of 0.5 g and 30 in./sec, respectively.

Six acceleration time histories were taken and capped at different percentages of peak acceleration to determine the effect of capping on their standardized displacements as shown in Figure 2. Because this figure shows that this effect is negligible, the proposed method uses the relationships developed by Franklin and Chang to estimate standardized displacements when acceleration levels are capped.

EXTERNAL STABILITY ANALYSIS

In the external stability analysis, a soil-reinforced wall supporting a sloping backfill as shown in Figure 3 is considered. The path of the failure plane shown in this figure passes underneath the wall, through the backfill at an angle θ, and then passes vertically until it intercepts the surface of the backfill. The vertical extent of this failure plane is dependent upon the cohesion of the backfill. Although it is common for the embedment lengths to be the same throughout the height of the wall, the angle β shown in Figure 3 allows for the modeling of uniformly changing lengths. The equations derived in this study assume a positive angle β.

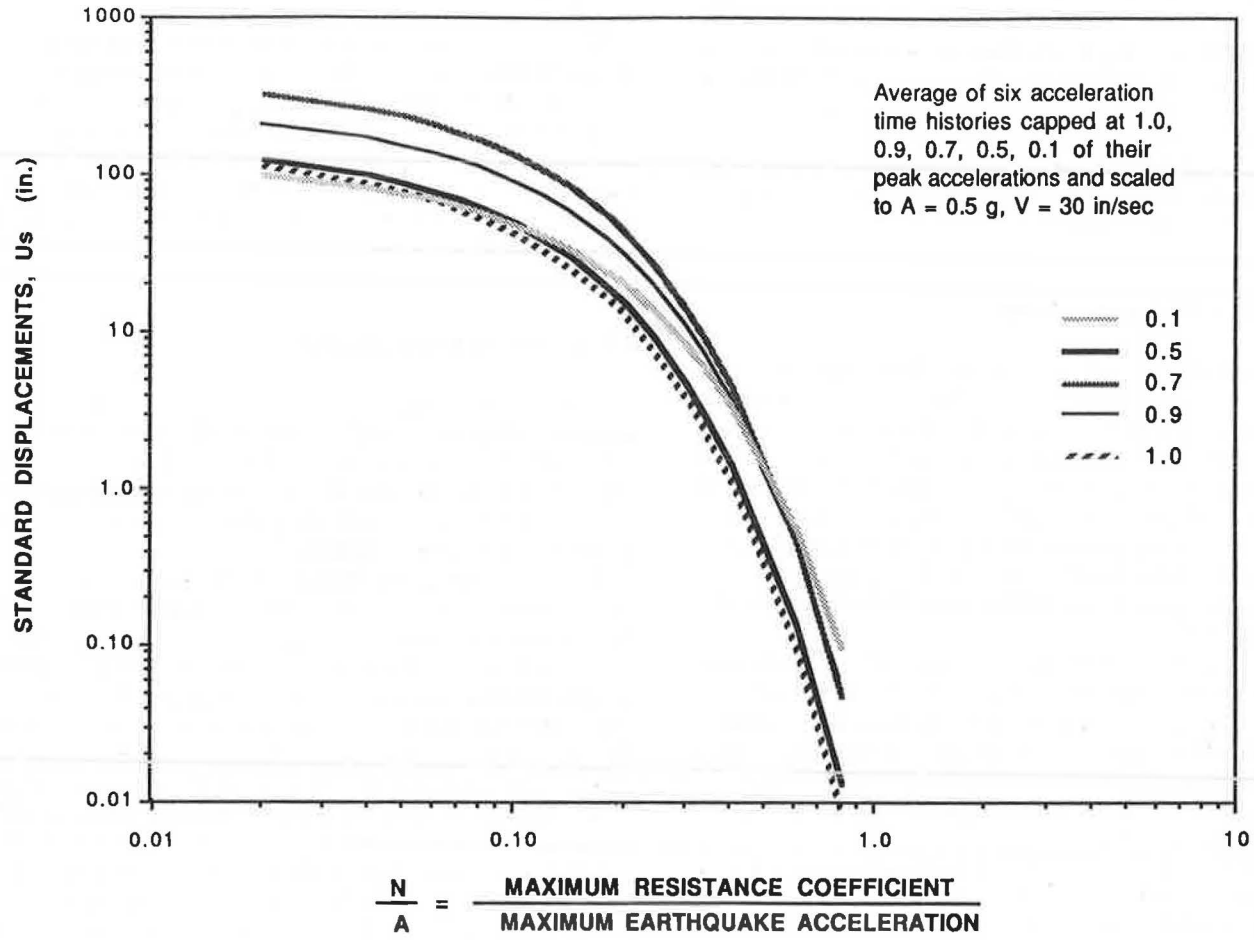

Note: N represents the critical acceleration, which is the acceleration required to reduce the factor of safety to unity.

FIGURE 2 Effect of capping acceleration histories on U_s and values of N/A (*9*).

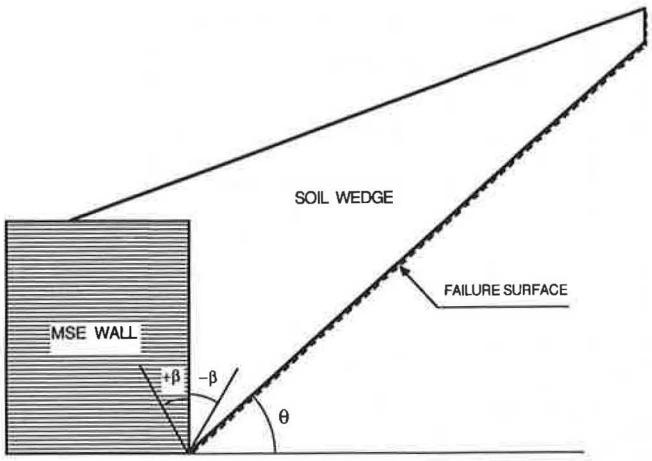

FIGURE 3 External stability analysis of wall and backfill.

A freebody diagram of the wall and the associated forces are shown in Figure 4. In this figure, W_1 represents the weight of the wall including the weight of the sloping backfill directly above it; K_n is the coefficient of acceleration applied in the horizontal direction; C_w and C_a are the forces developed due to cohesion at the wall interfaces; P is the force required for equilibrium of the wedge representing the sloping backfill; N_1 is the resultant force while ϕ_1 and ϕ_2 are the soil's internal friction angles at the wall/foundation and backfill interfaces.

The factor of safety against sliding of the wall, FS_s, is defined by Equation 1.

$$FS_s = \frac{F_r}{F_d} \tag{1}$$

where F_d and F_r represent the driving and resisting forces which are in turn defined as follows:

$$F_d = K_h W_1 + P\cos(\phi_2 + \beta) - C_a \sin\beta \tag{2}$$

$$F_r = C_w + \tan\phi_1 [P\sin(\phi_2 + \beta) + W_1 + C_a\cos\beta] \tag{3}$$

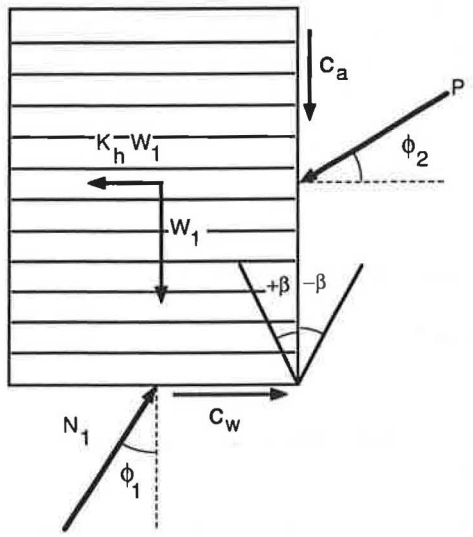

FIGURE 4 Wall freebody and associated forces.

The force P required for equilibrium of the backfill wedge is determined by considering the freebody diagram and the associated forces resolved in a force diagram as shown in Figure 5. In this figure C_L and C_a represent the cohesion forces developed over the lengths shown. The following equation for P is derived by resolving the forces in their horizontal and vertical components and back substituting:

$$P = \frac{B\sin(\theta - \phi_2) - A\cos(\theta - \phi_2)}{\cos(2\phi_2 + \beta - \theta)} \tag{4}$$

where

$$A = C_L\cos\theta - C_a\sin\beta - K_h W_2 \tag{5}$$

$$B = W_2 - C_a\cos\beta - C_L\sin\theta \tag{6}$$

The failure plane's angle of inclination, θ, is varied until the maximum value of P is found. This angle decreases with increasing levels of horizontal acceleration as shown in Figure 6.

The manner in which the external stability of a soil-reinforced wall is determined is similar to the Mononobe-Okabe method (*10,11*) of analyzing the dynamic stability of gravity retaining walls since both are extensions of the Coulomb-Rankine sliding wedge theory. Therefore, comparisons were made between the two methods in terms of $K_{ae}\cos\delta$, which represents the active earth pressure coefficient, and the friction angle of the wall-soil interface. The comparison, shown in Figure 7, indicates that the two methods yield identical results. It should be pointed out that in traditional gravity retaining wall analyses, the friction angle of the wall-soil interface, δ, is taken as one-half of the soil's internal friction angle (i.e., $\phi/2$). In the soil-reinforced wall analysis, the full friction angle is considered at this interface because it is predominantly a soil-to-soil contact. The effect is a reduction in the value of K_{ae} which is also shown in Figure 7.

INTERNAL STABILITY

Assumed Failure Plane

In the internal stability analysis, the factors of safety against yield and pullout of the reinforcement are determined for different levels of horizontal acceleration. In this determina-

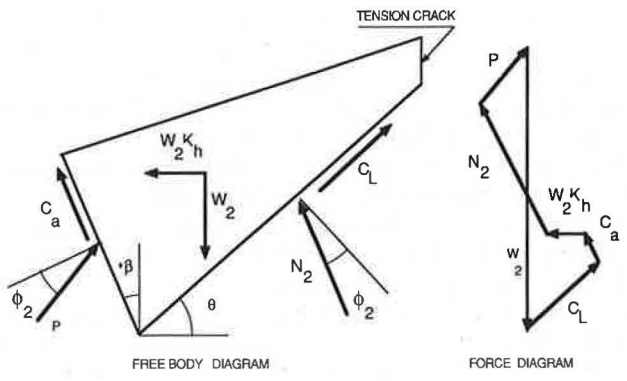

FIGURE 5 Backfill wedge freebody and force diagram.

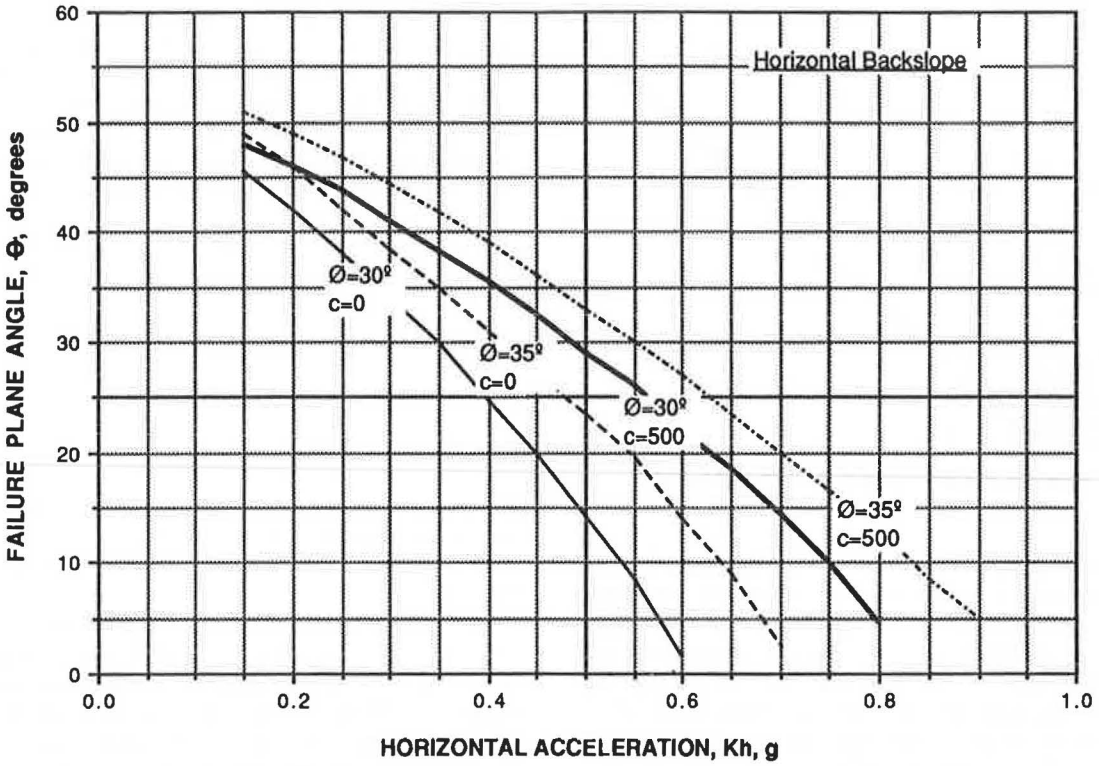

FIGURE 6 Variation of inclination of failure plane with horizontal acceleration.

tion, an assumption has to be made regarding the location and shape of the internal failure plane. Previous studies (*13–15*) analyzing the static behavior by instrumenting prototype walls have indicated that the failure surface starts near the toe and propagates upward in a parabolic manner.

In this study, the internal failure surface is held constant at (45 + ϕ/2) for both the static and dynamic load conditions. It is possible that during dynamic loading, the location and shape of the failure surface changes from the location and parabolic shape observed in the static condition. Because of the dynamic interaction of the reinforcement with the soil, it is assumed that this change is small and that it does not materially affect the tie force evaluation.

Dynamic Tie Force Evaluation

The method used to derive the equation for the total tie force at any level of reinforcement is similar to the derivation of the static tie force by Binquet (*16*). The individual tie forces are calculated by considering the element bounded by line segments marked *ABCD* and enveloping the *i*th tie as shown in Figure 8. Also, shown in this figure is a freebody diagram of the element, where T represents the tie force assumed to be inclined at the same angle as the failure plane; R represents the resultant force on the element's failure plane inclined at an angle ϕ_1, the soil's internal friction angle; and C represents the force developed along the length of the element's failure plane due to cohesion of the backfill material. Cohesion is represented in the derivation of the total tie force because slightly cohesive soils are now used as backfill material in soil-reinforced walls (*17*). The assumption of the tie force's inclination is not critical to the method. Identical values of tie force are determined whether the force is assumed to act horizontally or inclined for $\phi_1 = 30$ degrees. Slightly different values are determined for a ϕ_1 other than 30 degrees.

In this study, the total force (dynamic plus static) is equal to the mass of the active wedge, as defined by the assumed failure plane, multiplied by the horizontal acceleration. This total force is proportionally distributed to each tie depending on the area of the active wedge enveloped by each tie. The numbered forces in Figure 8 represent the internal and external body forces. The vertical and horizontal components of all the forces shown in this figure are listed in Table 1.

By summing these forces, back substituting and solving for T, the tie force at the ith level shown in Equation 7 is found.

$$T_i = \frac{K_h MF - MV - CG}{G} \tag{7}$$

where

$$M = \gamma \Delta H^2 (\tan \theta)^{-1}$$
$$V = (i - N - 1/2)$$
$$G = 2\sin \theta$$
$$F = (i - 1/2)\tan \theta$$

Comparison With Rankine's Active Earth Pressure Coefficient

The tie force determined in the foregoing manner can be compared to the force determined using Rankine's active earth

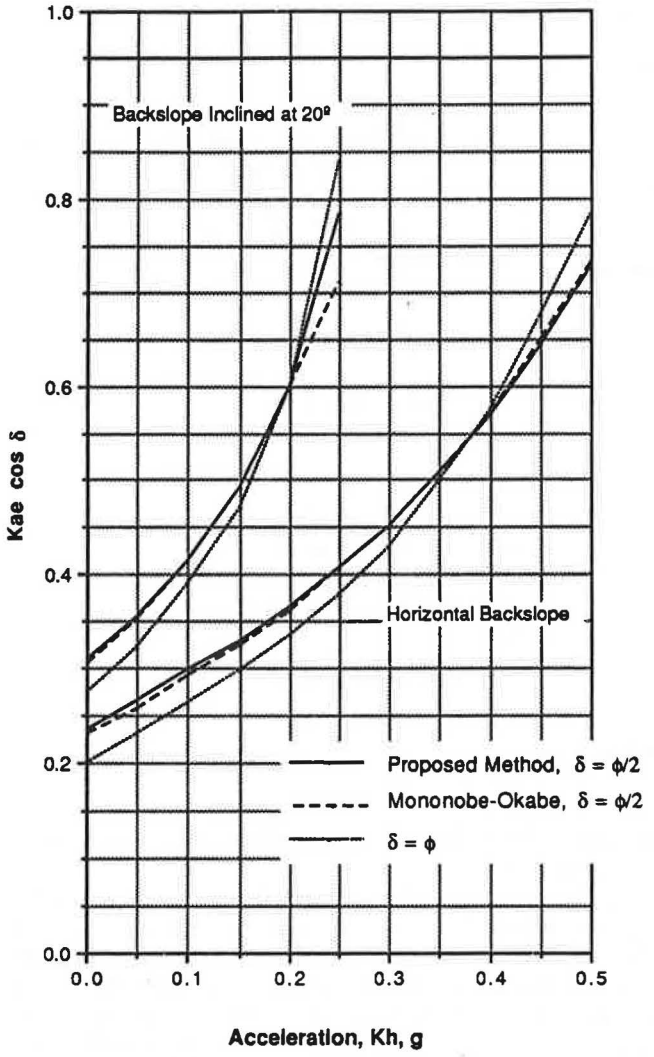

FIGURE 7 Comparison of dynamic earth pressure coefficients [after Seed and Whitman (*12*)].

pressure coefficient by setting the values of horizontal acceleration, K_h, and cohesion, C, equal to zero in Equation 7. When this is done, the absolute value of the tie force at any level is expressed as follows:

$$T_i = \frac{MV}{G} \tag{8}$$

Substituting the previously defined expressions for the values in Equation 8, the tie force is found to be:

$$T_i = Ka_1\gamma\,(N - i + 1/2)\Delta H^2 \tag{9}$$

where

$$Ka_1 = \frac{\sin(45 - \phi/_2)}{2\cos^2(45 - \phi/_2)}$$

When the tie force is calculated using Rankine's formula, the following relationship is derived:

$$T_i = Ka_2\,\gamma\,(N - i + 1/2)\Delta H^2 \tag{10}$$

where Ka_2 is equal to $\tan^2(45 - \phi/2)$, Rankine's active earth pressure coefficient.

The variation of the two coefficients, Ka_1 and Ka_2, is shown in Figure 9 as a function of friction angle. This figure shows that the methodology used results in slightly lower coefficients than the Rankine coefficients for friction angles less than 30 degrees, while the opposite is true for angles greater than 30 degrees.

Determination of Factors of Safety Against Yield and Pullout

Having determined the static and dynamic forces in the ties at all levels of embedment, the factors of safety against yield and pullout are determined next. The factor of safety against yield, FS_y, and against pullout, FS_p, are defined in the following equations:

$$FS_y = \frac{R_y}{T} \tag{11}$$

$$FS_p = \frac{R_p}{T} \tag{12}$$

where R_y and R_p are the respective resistances to yield and pullout of the ties per lineal foot of wall and T is the tie force per lineal foot. The results of laboratory and field pullout tests have commonly been reduced to a soil-reinforcement friction factor. In these tests, the friction factor, f, is determined by the following equation:

$$f = \frac{R_p}{P_v P_s EL} \tag{13}$$

where P_v is the vertical or overburden pressure, P_s is the perimeter of the reinforcing per lineal foot of wall, and EL is the embedment length behind the failure plane.

Values of friction factor as a function of overburden for different types of reinforcement and soil conditions are shown in Figure 10. The values were determined from both field and laboratory tests. Because the friction factor values have been shown to depend upon a number of factors like soil type, density, shear strength, and type of reinforcement, the pullout resistance for a given set of conditions would ideally be determined by field tests. In the absence of this type of data, the values shown in Figure 10 can be used.

In this study, Equation 13 is used to derive pullout resistance, R_p, at any level of reinforcement. In this equation, the values for P_v and EL, using the notation in Figure 8, are shown in Equations 14 and 15, respectively.

$$P_v = \gamma\Delta H(N - i + 1/2) \tag{14}$$

$$EL = OL - (\Delta H^* i/\tan\theta) \tag{15}$$

The soil-reinforcement friction factor, f, is modeled as a function of overburden pressure or level of reinforcement as shown in Equation 16.

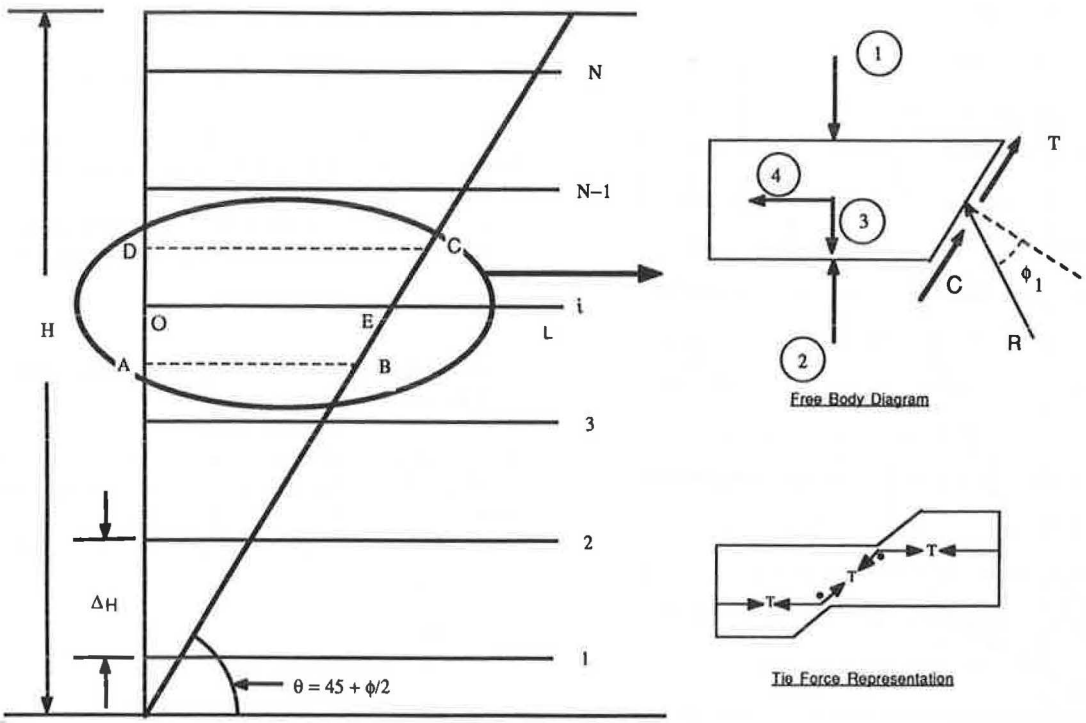

FIGURE 8 Representation of forces used to derive the total tie force.

TABLE 1 VERTICAL AND HORIZONTAL COMPONENTS OF FORCES SHOWN IN FIGURE 8

Force	Vertical	Horizontal
1	$-\gamma\Delta H^2(N-i)(i)\tan\theta^{-i}$	
2	$+\gamma\Delta H^2(N-i+1)(i-1)\tan\theta^{-1}$	
3	$-\gamma\Delta H^2(i-1/2)\tan\theta^{-1}$	
4		$-K_h\,\gamma\Delta H^2(i-1/2)\tan\theta^{-1}$
T	$+T_i\sin\theta$	$+T_i\cos\theta$
R	$+R_i\cos(\theta-\phi)$	$-R_i\sin(\theta-\phi)$
C	$+C\sin\theta$	$+C\cos\theta$

$$f_i = B_1 + B_2e^{-P_v} - B_3e^{-2P_v} \quad (16)$$

where B_1, B_2, and B_3 are constants obtained by solving three equations having friction values and corresponding overburden pressures in Kips obtained from either actual field/laboratory tests or the most applicable data shown in Figure 10.

Comparison With Previous Investigations

A computer program was written to perform the computations incorporating the proposed seismic design procedure (*18*). Data on the performance and behavior of a soil-reinforced wall during a seismic event is not known to exist. In view of this, the computer program was used to make predictions for tie forces and wall displacements for the 20-ft-high wall constructed and tested by explosives in the investigation by Richardson et al. (*4*).

In his investigation, Richardson placed explosives in front of the wall and 25 to 50 ft behind the wall at varying depths. The cumulative effect of a series of explosions in front of the wall resulted in a negligible total outward movement of 0.02 in., measured 6.3 ft below the top of the wall. In this series, the largest peak acceleration recorded at the base was 0.21 g, which was used as input to the computer program. The reinforcing used in construction of the wall consisted of longitudinal ties 80 mm wide and 3 mm thick. Because this type of reinforcing is similar to that used in establishing the curve for the smooth strips shown in Figure 10, a friction factor of 0.62 was input to determine the pullout resistance. Using the same soil and geometric properties of the wall, the model predicted no outward movement. The lowest factors of safety against yield, pullout, and sliding at the base were 5.9, 1.3, and 7.7, respectively.

The model predicted initiation of wall movements by sliding at the base at an acceleration of 0.6 g. At this level of acceleration, the factors of safety against pullout were less than unity for the upper four levels of reinforcement. The model predicted that the resistance to pullout at these levels would be exceeded at an acceleration of 0.43 g. The lowest factor of safety against yield was 5.5.

A series of explosives detonated behind the wall using larger amounts of dynamite produced base accelerations in excess of 0.8 g and resulted in a cumulative outward wall movement of 1.25 in. To quantify the displacements predicted by the model, it was noted that the explosive tests resulted in a single cycle of acceleration having a period generally less than 0.1 sec. Using this as a basis, a cumulative displacement of 0.62 in. was predicted.

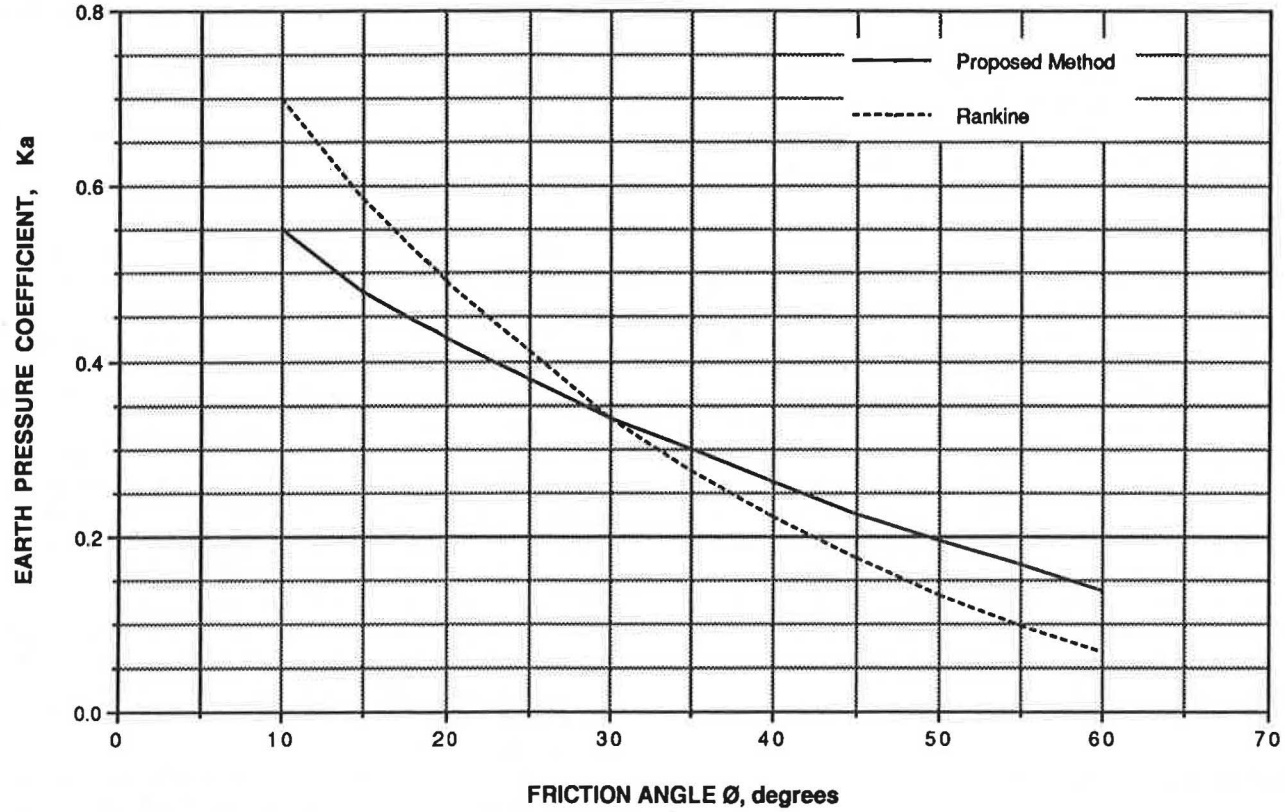

FIGURE 9 Comparison of Rankine active earth pressure coefficients.

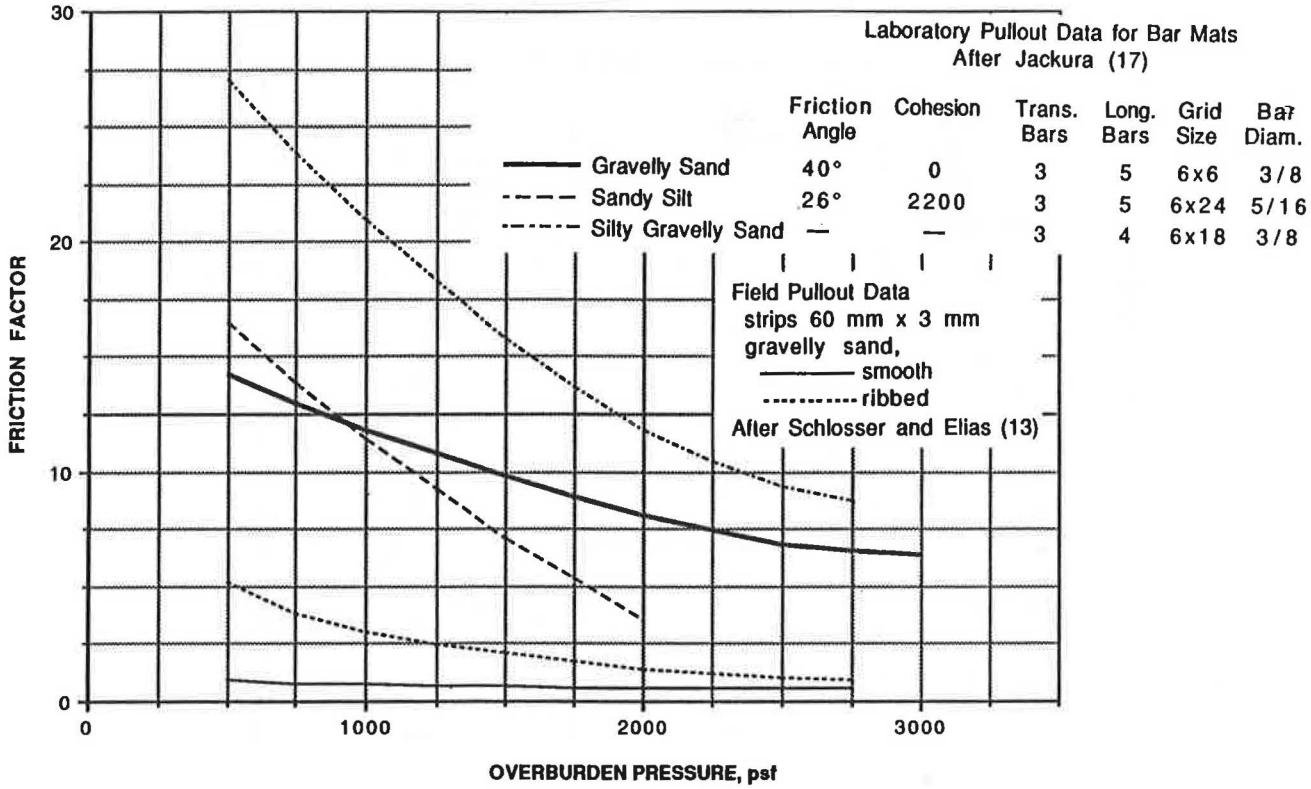

FIGURE 10 Variation of friction factor with overburden for different reinforcing elements and soil types.

Dynamic tie forces were also recorded and reported for an event that produced a peak acceleration of 0.08 g at the base. A comparison of these forces and the forces predicted by the model is shown in Figure 11. Also shown are the force levels predicted by the seismic design methodology based on the small-scale laboratory model studies. From this comparison it can be seen that the model predicts force levels approximately half-way between the explosive and laboratory model test results.

The observed cumulative displacement of the prototype wall is larger than what the model predicted. Because the primary effect of a blast is to move the wall outward, it is speculated that detonation of explosives behind the wall resulted in larger displacements than those caused by equivalent levels of acceleration applied at the base. This speculation is supported by the fact that the model overestimated the tie forces and correctly predicted the negligible observed displacement for the series of explosives detonated in front of the wall, while the model underestimated the displacements resulting from the explosive series placed behind the wall.

However, the model predicted relatively small displacements for events resulting in large levels of acceleration, while, similarly, small wall displacements were observed. This fact should not be overlooked.

PRACTICAL APPLICATION

The proposed seismic design was used to determine permanent displacements due to different earthquake loads for the 62-ft-high wall described in a companion paper by Jackura, elsewhere in this Record. The wall's site seismic parameters are controlled by the Maacama Fault. It is postulated, based on the fault's distance from the site, that the peak bedrock accelerations for the maximum credible (M7.5) and probable (M5.0) events are 0.7 g and 0.5 g, respectively.

The wall's overall dimensions and reinforcing type were entered into the computer program along with the applicable soil strengths for both the wall itself and the soil behind it. The upper curve shown in Figure 10 was selected to estimate the pullout resistance because the reinforcement is a bar-mat and the soil used to construct the wall approximates the soil for this curve.

For the external analysis, the variation of the factor of safety against sliding at the wall base with acceleration, as determined by the program, is shown in Figure 12. This figure shows the factor of safety dropping below unity at a level of acceleration greater than 0.49 g. No permanent displacement is predicted, therefore, for the postulated maximum probable seismic event producing 0.5 g at the site. For a peak acceleration of 0.7 g representing the maximum credible event, a permanent displacement of approximately 1 in. is predicted, which is considered well within tolerable limits.

The internal stability analysis is limited to considering peak accelerations up to and not exceeding 0.49 g, because sliding at the wall base is predicted to occur at that level. Therefore, any consideration of an acceleration time history for this analysis is capped at 0.49 g.

The variation of factors of safety against reinforcement pullout and yield with acceleration at three different levels of wall height is shown in Figure 13. This figure shows the factor of safety against pullout approaching unity for the top level of reinforcement while the factor of safety against yield approaches a value of 3 at the higher levels of acceleration for each of

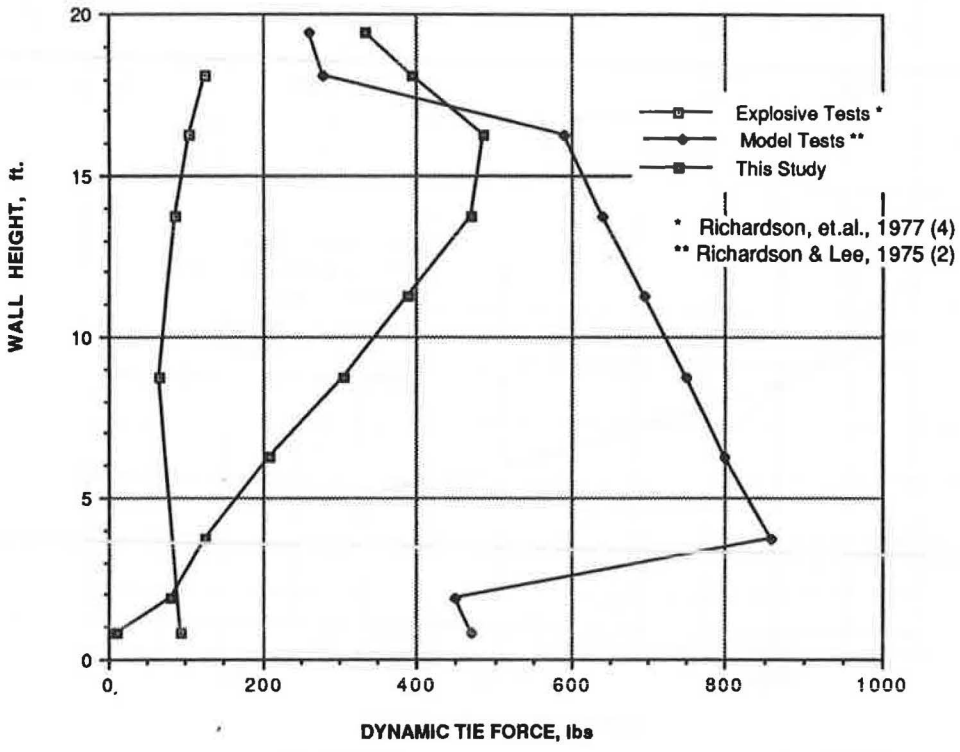

FIGURE 11 Comparison of dynamic tie forces, maximum base acceleration of 0.08 g [after Richardson et al. (*4*)].

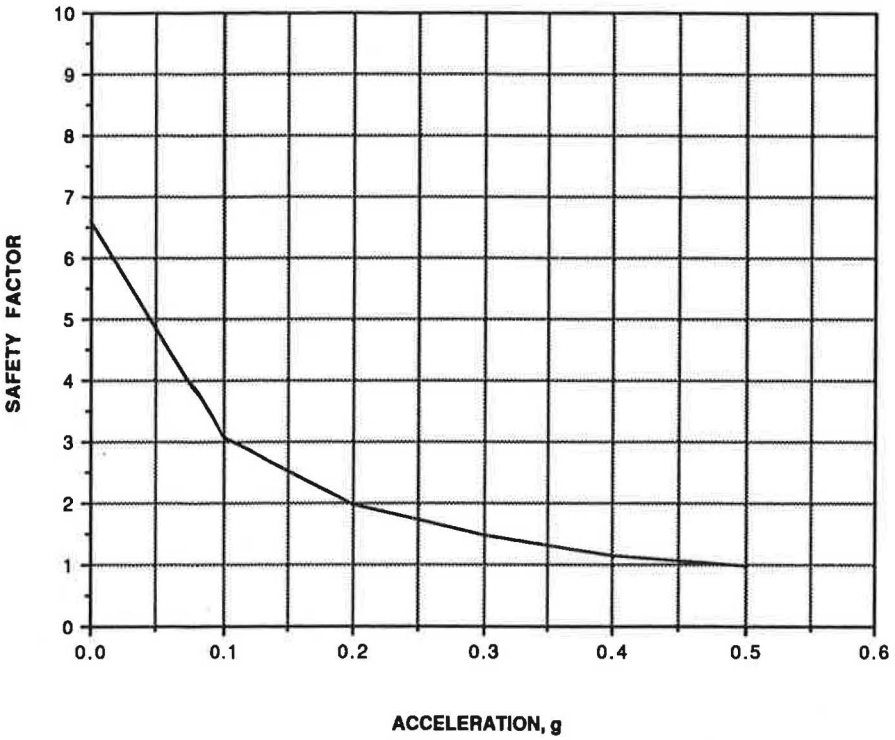

FIGURE 12 Influence of acceleration on the factor of safety against the wall sliding along its base.

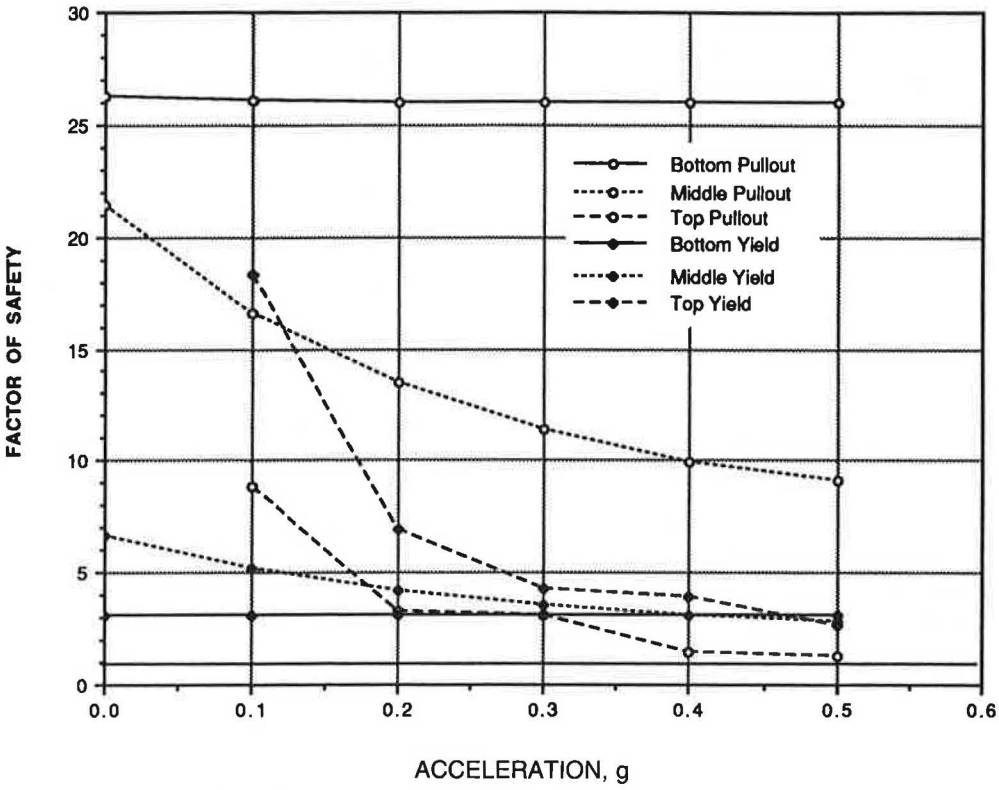

FIGURE 13 Variation of factor of safety against yield and pullout with acceleration for three levels of reinforcement.

the three levels of reinforcement. The factors of safety against yield shown in Figure 13 do not account for the effects of corrosion. Over the period of the wall's service life it is estimated that the reinforcement's cross-sectional area will be reduced by 50 percent due to corrosion. This would then reduce the yield factor of safety to 1.5 at 0.5 g, which is still sufficient to preclude the breaking or rupture of the reinforcement.

Based on the results of this analysis, the wall's design was considered adequate and the permanent displacements considered to be well within tolerable limits.

SUMMARY AND CONCLUSIONS

The proposed method described in this paper determines the factors of safety as a function of horizontally applied acceleration for both the external and internal stability of a soil-reinforced wall. The method was used to predict the performance of a 20-ft-high wall tested dynamically by explosive charges. The method's prediction compared favorably with the wall's observed behavior by predicting the level of acceleration at which movement would be initiated.

The method was then used to check the design and predict the performance of a 62-ft-high wall constructed in northern California. The design was found to be adequate and negligible permanent displacements were predicted for the postulated maximum credible seismic event.

It can be concluded that the method indicates initiation of sliding along a wall base at the higher levels of acceleration and that the upper layers of reinforcement are the most susceptible to pullout. This susceptibility to pullout can be mitigated by increasing the length of the reinforcement. Perhaps most importantly, the method indicates very small permanent displacement for Caltrans's current design of soil-reinforced walls under very severe seismic loading conditions.

Caltrans sponsors research at the University of California at Davis to verify and improve the method described. The research consists of testing model walls under both static and dynamic loads in the centrifuge. Preliminary results appear to validate the method and the assumptions used.

ACKNOWLEDGMENTS

A number of individuals on the Caltrans staff contributed to the development of the proposed methodology. Thang Le and Cuong Nguyen performed analyses and wrote portions of the computer program. Peter Dirrim performed analyses on the effect of capping acceleration time histories on their standardized displacements. Bruce Hartman combined the many elements of computer code and made the program user friendly. Their efforts, skills, and enthusiasm are acknowledged and greatly appreciated.

REFERENCES

1. H. Vidal. The Principle of Reinforced Earth. In *Highway Research Record 282*. HRB, National Research Council, Washington, D.C., 1969, pp 1–16.
2. G. N. Richardson and K. L. Lee. Seismic Design of Reinforced Earth Walls. *Journal of the Geotechnical Engineering Division*, ASCE Vol. 101, No. GT2, Feb. 1975, pp 167–188.
3. W. E. Wolfe, K. L. Lee, D. Rea, and A. M. Yourman. The Effect of Vertical Motion on the Seismic Stability of Reinforced Walls. *Proc., ASCE Symposium of Earth Reinforcement*, Pittsburgh, Pa. April 27, 1978.
4. G. N. Richardson, D. Feger, A. Fong, and K. L. Lee. Seismic Testing of Reinforced Earth Walls. *Journal of the Geotechnical Engineering Division*, ASCE Vol. 103, No. GT1, Jan. 1977, pp 1–17.
5. G. N. Richardson. Earthquake Resistant Reinforced Earth Walls. *Proc., ASCE Symposium on Earth Reinforcement*, Pittsburgh, Pa., April 17, 1978.
6. D. P. McKittrick and L. J. Wojciechowski. Design and Construction of Seismically Resistant Reinforced Earth Structures. *Proc., International Conference on Soil Reinforcement: Reinforced Earth and Other Techniques*. Vol. I, Paris, March 1979.
7. N. M. Newmark. Effects of Earthquakes on Dams and Embankments. *Geotechnique*, Vol. 15, No. 2, Jan. 1965.
8. R. Richards and D. G. Elms. Seismic Behavior of Gravity Retaining Walls. *Journal of the Geotechnical Engineering Division*, ASCE Vol. 105, No. GT4, April 1979, pp 449–464.
9. A. G. Franklin and F. K. Chang. Earthquake Resistance of Earth and Rockfill Dams. *Report 5: Permanent Displacements of Earth Embankments by Newmark Sliding Block Analysis*. Miscellaneous Paper S-71-17, Soils and Pavements Laboratory, U.S. Army Engineer Waterways Experiment Station, Vicksburg, Miss., Nov. 1977.
10. N. Mononobe and U. Matsuo. On the Determination of Earth Pressure During Earthquakes. *Proc., Ist World Conference on Earthquake Engineering*, Tokyo, Vol. 9, 1929.
11. S. Okabe. General Theory of Earth Pressure and Seismic Stability of Retaining Wall and Dam. *Journal of the Society of Civil Engineers*, Vol. 12, N1, 1920.
12. H. B. Seed and R. V. Whitman. Design of Earth Retaining Structures for Dynamic Loads. *Proc., ASCE Conference on Lateral Stresses, Cornell University*, Ithaca, N.Y., June 1970, pp 103–147.
13. F. Schlosser and V. Elias. Friction in Reinforced Earth. *Proc., ASCE Symposium on Earth Reinforcement*, Pittsburgh, Pa., April 27, 1978.
14. I. Juran, F. Schlosser, N. T. Long, and G. Legeay. Full Scale Experiment on a Reinforced Earth Bridge Abutment in Lille. *Proc., ASCE Symposium on Earth Reinforcement*, Pittsburgh, Pa., April 27, 1978.
15. U. Dash. Design and Field Testing of a Reinforced Earth Wall. *Proc., ASCE Symposium on Earth Reinforcement*. Pittsburgh, Pa., April 27, 1978.
16. J. Binquet. Analysis of Failure of Reinforced Earth Walls. *Proc., ASCE Symposium on Earth Reinforcement*, Pittsburgh, Pa., April 17, 1978.
17. K. Jackura. Results of Minor Research on Bar-Mat Pullout Tests. Office of Transportation Laboratory, California Department of Transportation, May 1984.
18. California Department of Transportation. DYNMSE–Computer Program to Evaluate the Dynamic Stability of MSE Walls. Office Report, July 1988.